Chapter

Bismuth Halide Perovskites for Photovoltaic Applications

Khursheed Ahmad

Abstract

In the last decade, energy crisis has become the most important topic for researchers. Energy requirements have increased drastically. To overcome the issue of energy crisis in near future, numerous efforts and sources have been developed. Therefore, solar energy has been considered the most promising energy source compared to other energy sources. There were different kinds of photovoltaic devices developed, but perovskite solar cells have been considered the most efficient and promising solar cell. The perovskite solar cells were invented in 2009 and crossed an excellent power conversion efficiency of 25%. However, it has a few major drawbacks, such as the presence of highly toxic lead (Pb) and poor stability. Hence, numerous efforts were made toward the replacement of Pb and highly stable perovskite solar cells in the last few years. Bismuth halide perovskite solar cell is one type of the replacement introduced to overcome these issues. In this chapter, I have reviewed the role of bismuth halide perovskite structures and their optoelectronic properties toward the development of perovskite solar cells.

Keywords: methyl ammonium bismuth halide, perovskites, light absorbers, photovoltaics, perovskite solar cells

1. Introduction

In the last few decades, researchers/scientists have focused to find out the most efficient and promising technology to fulfill the energy requirements globally [1–7]. There are various renewable energy sources, but solar energy is a never-ending source. Photovoltaic or solar cell is a device that converts solar energy into electrical energy. In 2009, perovskite solar cells (PSCs) were developed, which exhibited the good open circuit voltage with decent power conversion efficiency (PCE) [6]. The term "perovskite" was created for calcium titanate ($CaTiO_3$) by Russian mineralogist L.A. Perovski [6]. However, another class of perovskite has also been discovered with molecular formula of ABX_3, where A = organic or inorganic cation such as $CH_3NH_3^+$ or Cs^+, B=Pb^{2+} or Sn^{2+}, etc. and X = halide anions. Miyasaka and co-workers have prepared methyl ammonium lead halide ($MAPbX_3$; MA = $CH_3NH_3^+$, X = I^- or Br^-) perovskites and used as visible light sensitizer in dye-sensitized solar cells (DSSCs) [6]. The fabricated device showed an interesting PCE of 3%. However, the use of liquid electrolyte destroyed its photovoltaic performance due to the dissolution of $MAPbX_3$ in the liquid electrolyte. Later, various strategies were developed to solve this issue, and a solid-state hole transport material was employed to overcome the dissolution of perovskites [8–19]. Later, some other strategies were made to further enhance the photovoltaic parameters of the perovskite solar cells. Lee et al. in 2012 reported

an improved PCE of 10.9% by introducing solid-state perovskite solar cells [20]. In a short span of time, perovskite solar cells attracted researchers globally. In 2019, the highest PCE of 23.3% was reported for Pb halide perovskite solar cells [21]. This enhanced PCE is really impressive and has the potential for practical applications of perovskite solar cells. $MAPbX_3$ has also been used in other applications such as photodetectors, light-emitting-diodes, batteries and supercapacitors due to the presence of excellent optoelectronic properties in the perovskite materials [22–26]. $MAPbX_3$ has been considered the key material for the development of high-performance perovskite solar cells due to its excellent absorption coefficient. $MAPbX_3$ perovskite worked as a light absorber in perovskite solar cells. However, the presence of highly toxic Pb in the $MAPbX_3$ structure is a major drawback and a challenge for the scientific community to replace it with less toxic or nontoxic element. The presence of toxic Pb also restricted the practical use of perovskite solar cells. Thus, in the last 5 years, Pb has been replaced with Sn and Ge and showed good performance, but poor stability dismissed their performance [27, 28]. The perovskite structures possess general formula of ABX_3 as discussed above. The optical properties of the perovskite materials can be tuned by changing the A, B or X ion present in the ABX_3 structure. The size of the A, B or X should satisfy the Goldschmidt tolerance factor (t) equation given below:

$$(\mathrm{t}) = \frac{(rA + rX)}{\sqrt{2}(rB + rX.)} \tag{1}$$

where rA and rB are ionic radii of the A and B, while rX is the ionic radii of the X present in the ABX_3 structure. The perovskite materials showed good stability when tolerance factor is equal to 1. Recently, bismuth (Bi), antimony and copper, which are less toxic metals, have been used for the fabrication of Pb-free perovskite solar cells [29–32]. The Bi is a nontoxic element and has the similar properties and ionic size to those of Pb. The ionic radii of the Bi also satisfy the tolerance factor rule and enhanced the stability of the Bi-based perovskite materials. Moreover, it was found that Bi-based perovskite materials possess higher absorption coefficient, which makes them an efficient light-absorbing material for solar cell applications. Thus, Johansson et al. employed a ternary Bi-based perovskites with a molecular formula of $A_3Bi_2I_9$ ($A = MA^+$ or Cs^+) for Pb-free perovskite solar cells [33]. Buonassisi et al. also employed solvent engineering approach using $A_3Bi_2I_9$ perovskite material and the PCE of 0.71% was obtained [34]. Later, various approaches have been made to improve the performance of the Bi-based perovskite solar cells, and the highest PCE of 3.17% was achieved by applying vapor deposition approach [35]. In this chapter, I have reviewed the fabrication of perovskite solar cells. Recent advances in Bi-based perovskite solar cells and future prospective have also been described.

2. Fabrication of perovskite solar cells

Generally, perovskite solar cells are composed of different components such as electrode substrates (usually indium-doped tin oxide [ITI] or fluorine-doped tin oxide [FTO] glass substrates), perovskite light absorber layer, electron transport layer, hole transport layer and metal contact layer. Firstly, FTO or ITO glass substrates were cleaned and patterned with zinc powder and 2 molar hydrochloride solution to avoid short circuit in the device. Further, an electron transport layer was spin coated and annealed at ~500°C. Further, perovskite layer was deposited and annealed at temperature of ~ 70–120°C. Later, a hole transport material (HTM) layer was deposited followed by the deposition of metal contact layer of Au or Ag using thermal evaporation. The fabrication of perovskite solar cells has been illustrated in **Figure 1**.

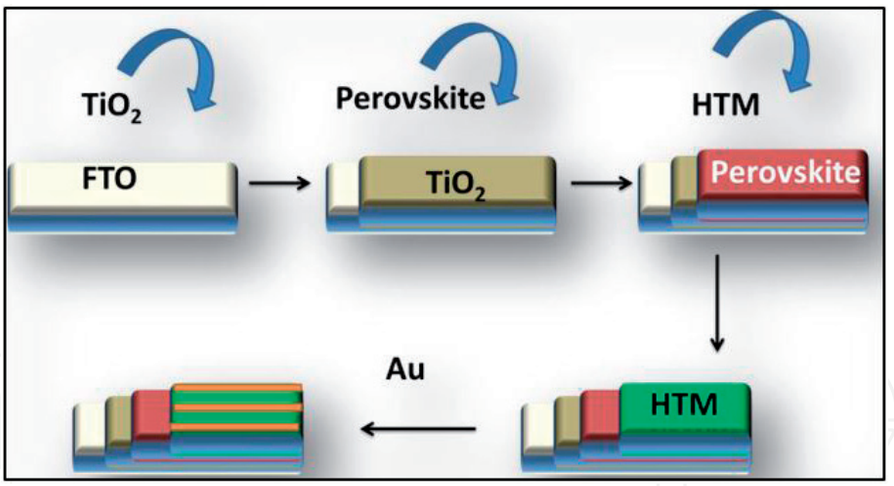

Figure 1.
Schematic illustration for the fabrication of perovskite solar cells.

The performance of the fabricated perovskite solar cells is investigated by various techniques such as photocurrent-voltage (I-V), external quantum efficiency (EQE), incident-photon-to-current-conversion efficiency (IPCE), photoluminescence spectroscopy, etc. Generally, the photovoltaic performance of any perovskite solar cells is estimated in terms of power conversion efficiency (PCE), fill factor, open circuit voltage and photocurrent density using I-V measurements. Photoluminescence spectroscopy revealed the electron lifetime of the generated electron in the perovskite structure, which is used to check the recombination reactions. It is believed that the perovskite solar cells with lower recombination reaction rate or high electron lifetime provide better performance in terms of efficiency.

3. Origin of bismuth halide perovskite solar cells

Since 2009, perovskite solar cells attracted enormous attention due to their excellent performance and simple fabrication process. However, the presence of highly toxic Pb remains a challenge. In recent years, bismuth has been employed to replace Pb from perovskite solar cells. Bismuth has been explored and Pb-free perovskite structures have been synthesized and employed for the development of Pb-free perovskite solar cells. Ahmad et al. employed new Pb-free perovskite light absorbers for perovskite solar cell applications [29–31]. The performance of these perovskite solar cells was less than 1%. In 2019, Lan et al. used $FA_3Bi_2I_9$ ($FA = CH(NH_2)_2$) perovskite material for perovskite solar cell applications [36]. In this work, the authors also prepared $MA_3Bi_2I_9$ ($MA = CH_3NH_3^+$) perovskite for perovskite solar cell applications. The X-ray diffraction (XRD) patterns of the $FA_3Bi_2I_9$ and $FA_3Bi_2I_9$ were found to be well-matched with the previous Joint Committee on Powder Diffraction Standards (JCPDS) data.

Ghasemi et al. [37] also prepared a new bismuth-based perovskite material phenethylammonium bismuth halides ($(PEA)_3Bi_2I_9$, $(PEA)_3Bi_2Br_9$ and $(PEA)_4Bi_2Cl_{10}$). The authors have prepared the crystal structures of these perovskite materials under facile conditions. The crystal structures of the $(PEA)_3Bi_2I_9$, $(PEA)_3Bi_2Br_9$ and $(PEA)_4Bi_2Cl_{10}$ have been presented in **Figure 2**. Furthermore, they have been investigated for their physiochemical properties for optoelectronic applications.

The crystal structures of $(PEA)_3Bi_2I_9$, $(PEA)_3Bi_2Br_9$ and $(PEA)_4Bi_2Cl_{10}$ showed the monoclinic crystal system with space group of $P2_1/n$, $P2_1/n$ and $P2_1/c$, respectively.

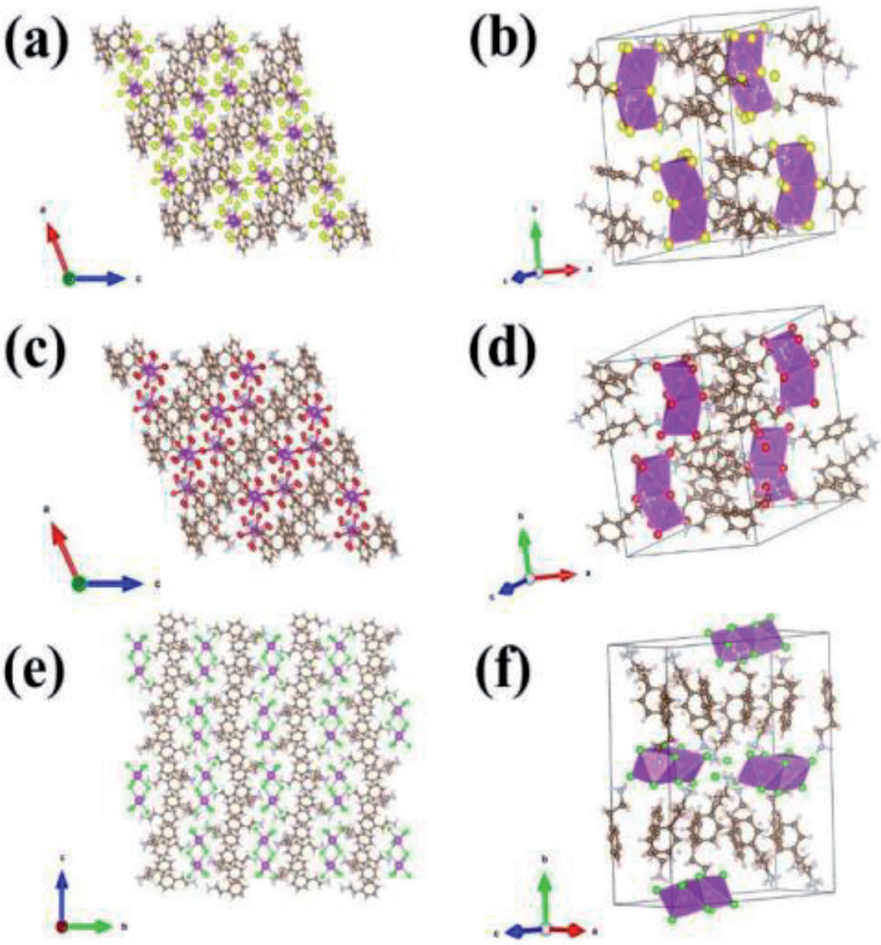

Figure 2.
Crystal structures of $(PEA)_3Bi_2I_9$ (a and b), $(PEA)_3Bi_2Br_9$ (c and d) and $(PEA)_4Bi_2Cl_{10}$ (e and f). Reproduced with permission [37].

These perovskite structures were composed of octahedral halide anionic clusters associated with PEA^+ cationic groups. In the crystal structures, Bi atom is situated in the center of each octahedron, whereas halide anions are in the corner of every face-sharing octahedron. The prepared perovskite structures possess zero-dimensional (0D) structure. The calculated XRD of $(PEA)_3Bi_2I_9$ from the single crystal structure and measured XRD of the powder sample have been presented in **Figure 3a**. The measured XRD of $(PEA)_3Bi_2I_9$ was well-matched with the calculated XRD pattern. The UV-vis spectra of the $(PEA)_3Bi_2I_9$, $(PEA)_3Bi_2Br_9$ and (PEA) have been plotted in **Figure 3b**. The band gap of the $(PEA)_3Bi_2I_9$, $(PEA)_3Bi_2Br_9$ and $(PEA)_4Bi_2Cl_{10}$ was calculated by Tauc relation as shown in **Figure 3c**. The direct band gap of the prepared $(PEA)_3Bi_2I_9$, $(PEA)_3Bi_2Br_9$ and $(PEA)_4Bi_2Cl_{10}$ perovskite structures was found to be 2.23, 2.66 and 3.28 eV, whereas indirect band gap was 2.38, 2.79 and 3.38 eV, respectively.

The UPS of the $(PEA)_3Bi_2I_9$ perovskite structure has been presented in **Figure 3d**, which provides better information of the energy levels of the $(PEA)_3Bi_2I_9$ perovskite structure. Further, perovskite solar cells were fabricated and cross-sectional scanning electron microscopic (SEM) image of the device has been presented in **Figure 4a**, whereas the photocurrent density (I)-voltage (V) curves have been depicted in **Figure 4b**. The SEM image showed the connection between the interlayers of the perovskite solar cell components. The I-V curves of the fabricated perovskite solar cells with $(PEA)_3Bi_2I_9$ and $(MA)_3Bi_2I_9$ perovskite light absorbers showed good open circuit voltage, but the performance was poor. The open circuit voltage of the $(PEA)_3Bi_2I_9$-based perovskite solar cell was high with improved

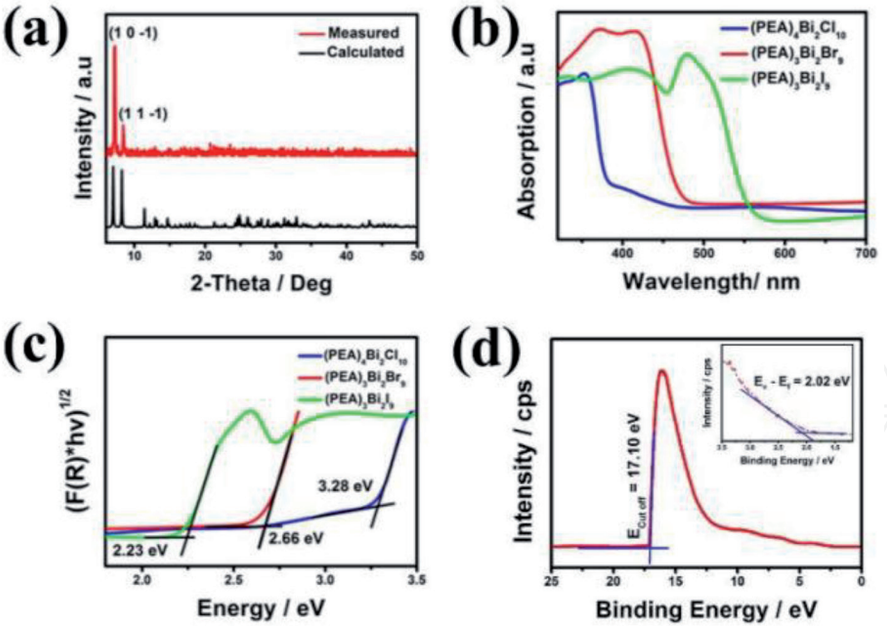

Figure 3.
Calculated and experimental XRD (a) of $(PEA)_3Bi_2I_9$, UV–vis spectra of $(PEA)_3Bi_2I_9$, $(PEA)_3Bi_2Br_9$ and $(PEA)_4Bi_2Cl_{10}$ (b), Tauc relation of $(PEA)_3Bi_2I_9$, $(PEA)_3Bi_2Br_9$ and $(PEA)_4Bi_2Cl_{10}$ (c) and ultraviolet photoemission spectroscopic (UPS) curve of $(PEA)_3Bi_2I_9$ (d). Reproduced with permission [37].

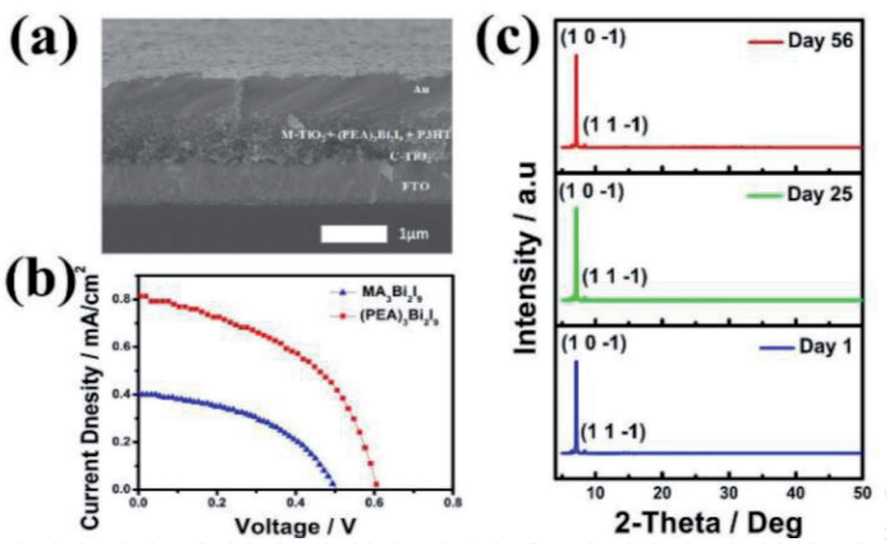

Figure 4.
Cross-sectional SEM images of perovskite solar cell device (a), I-V curve (b) of perovskite solar cells and XRD patterns of the $(PEA)_3Bi_2I_9$ perovskite structure exposed to air for different time. Reproduced with permission [37].

photocurrent density compared to the $(MA)_3Bi_2I_9$-based perovskite solar cells. The PCE of the $(PEA)_3Bi_2I_9$-based perovskite solar cells were found to be 0.23% with high open circuit voltage of 614 mV. However, the open circuit voltage for the $(MA)_3Bi_2I_9$-based perovskite solar cell was found to be 515 mV with PCE of 0.09%. The obtained results were found to be poor in terms of PCE.

Kulkarni et al. [38] also developed the Pb-free perovskite solar cells using $(MA)_3Bi_2I_9$ perovskite structure with novel strategies. Kulkarni et al. have employed N-methyl pyrrolidone (NMP) additive as morphology controller. In this work, different amount of NMP was added to observe the effect of NMP on the surface morphology of $(MA)_3Bi_2I_9$ perovskite.

The XRD patterns of the $(MA)_3Bi_2I_9$ without and with different amount of NMP were recorded and the obtained results have been presented in **Figure 5**. The obtained XRD patterned was well-matched with previously reported JCPDS data. This confirms the formation of $(MA)_3Bi_2I_9$ phase. However, the addition of NMP increases the peak intensity, which resulted in the orientation change. The other parameters also suggested that addition of NMP increases the crystallinity of the $(MA)_3Bi_2I_9$. Therefore, it can be said that the prepared $(MA)_3Bi_2I_9$ perovskite in the absence of NMP has poor crystalline phase or poor crystallinity. Furthermore, to investigate the effect of NMP on the morphological features, SEM images were recorded and have been presented in **Figure 6**.

The SEM image of $(MA)_3Bi_2I_9$ without NMP (**Figure 6a**) showed the hexagonal flakes with high exposure of TiO_2 and nonuniform surface. However, in case of $(MA)_3Bi_2I_9$ with NMP 12.5% (**Figure 6b**) showed large crystals, but poor uniform surface was observed. When 25% NMP (**Figure 6c**) was added, the surface morphology further changed. And the addition of 50% NMP drastically changed the surface morphology with larger grains as shown in **Figure 6d**. This suggested that 12.5% NMP was not sufficient to control the surface morphology of the $(MA)_3Bi_2I_9$. Moreover, $(MA)_3Bi_2I_9$ with 25% NMP covers the whole surface of the electrode substrate uniformly.

Further, perovskite solar cells were fabricated using $(MA)_3Bi_2I_9$ without and with NMP (at different percentage) under same conditions. The I-V and IPCE curves of the fabricated perovskite solar cells have been presented in **Figure 7a** and **b** respectively. The photocurrent density (J_{sc}) and PCE histograms were also presented in **Figure 7c** and **d**, respectively. The perovskite solar cell device fabricated in the absence of NMP showed PCE of 0.19% and open circuit voltage of 530 mV. However, the improved PCE of 0.31% was obtained for the perovskite solar cells fabricated with the addition of 25% NMP. In other cases, perovskite solar cells fabricated with 12.5% and 50% NMP showed lower performance, which may be due to the poor coverage of surface morphology.

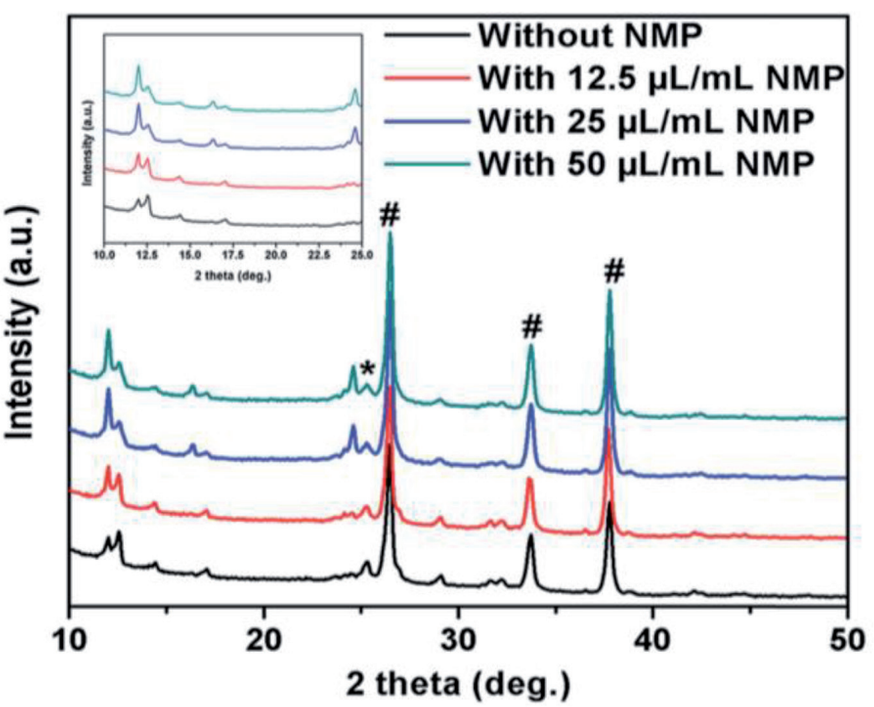

Figure 5.
*XRD of $(MA)_3Bi_2I_9$ without and with different amount of NMP. # peak for FTO and * for TiO_2. Reproduced with permission [38].*

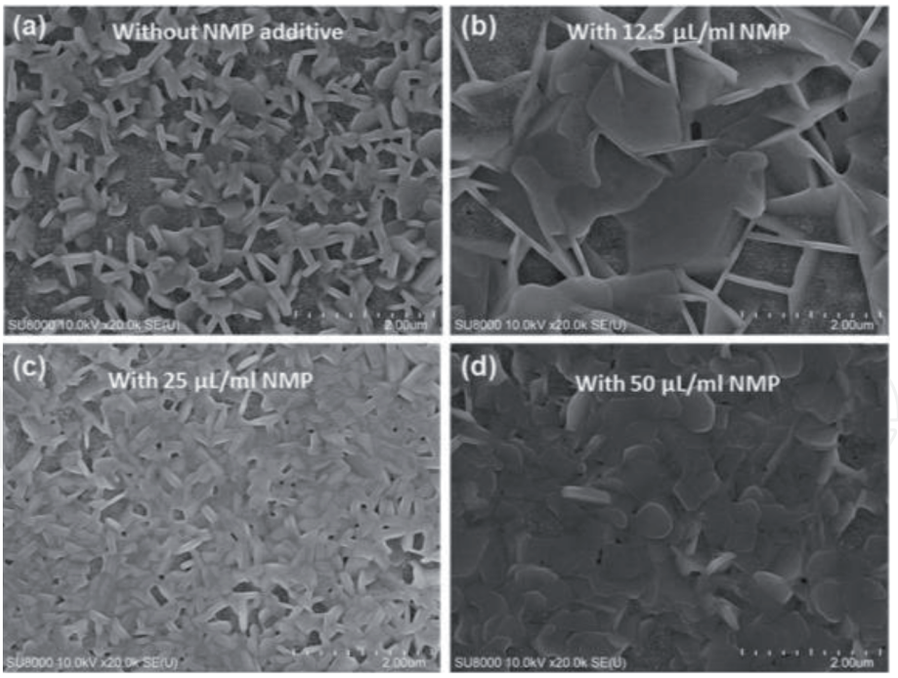

Figure 6.
SEM image of $(MA)_3Bi_2I_9$ without (a) and with different amount of NMP (b–d). Reproduced with permission [38].

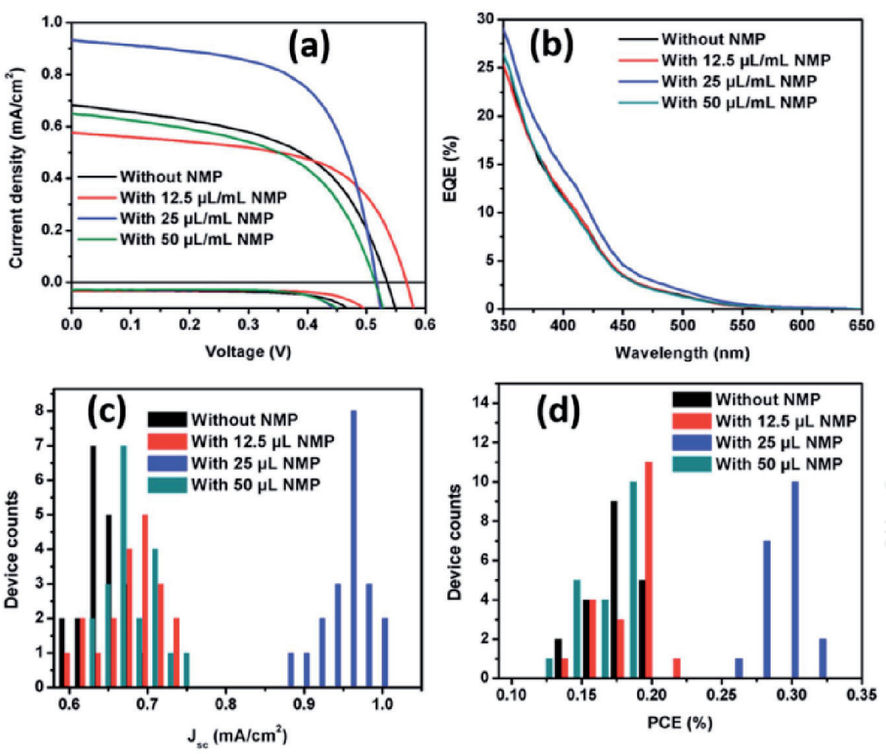

Figure 7.
Average I-V curves (a), IPCE (b), J_{sc} (c) and PCE (d) histogram of devices with and without NMP. Reproduced with permission [38].

In another work, Yu et al. [39] have prepared new perovskite solar cell device architecture of perovskite solar cells with mixed halide bismuth-based perovskite light absorber.

The authors have prepared a series of mixed halide-based perovskite structures. They have employed novel and simple strategies to prepare the Pb-free perovskite

solar cells. The optical images of the $Cs_3Bi_2I_{9-x}Br_x$ perovskite series (x = 0, 1, 2, 3, 4, 6 and 9) have been presented in **Figure 8a**, which show the different colors of the prepared thin films, and this change in the color of the perovskite thin film was due to the change in the halide composition. Further, optical properties were checked by recording absorption spectra of the prepared thin films of $Cs_3Bi_2I_{9-x}Br_x$ perovskite series (x = 0, 1, 2, 3, 4, 6 and 9). The band gap of the $Cs_3Bi_2I_9$ was lower than that of the $Cs_3Bi_2Br_9$ as confirmed by the absorption spectra (**Figure 8b**).

The XRD patterns of the $Cs_3Bi_2I_{9-x}Br_x$ perovskite series (x = 0, 1, 2, 3, 4, 6 and 9) have been presented in **Figure 8c**. The obtained results showed strong and well-defined diffraction peaks, which suggested the high crystalline nature of the prepared Pb-free perovskite structures. The obtained XRD results were well-matched with previous JCPDS card number 23-0847. This confirms the successful formation of the prepared Pb-free perovskite structures. Further, perovskite solar cell devices were fabricated with these perovskite light absorbers. The schematic graph for the energy level values of the Pb-free perovskite solar cell components has been displayed in **Figure 9a**.

The schematic diagram showing that the electrons generated in the perovskite structure is transferred to the hole transport layers. The cross-sectional SEM image of the fabricated perovskite solar cells showed all the component layers of the perovskite solar cells in **Figure 9b**. Further, perovskite solar cells were fabricated by using different light absorbers $Cs_3Bi_2I_9$ and $Cs_3Bi_2I_6Br_3$. The I-V measurements (**Figure 10a**) and external quantum efficiency (EQE) were measured (**Figure 10b**) of the fabricated perovskite solar cells. The I-V curve of the $Cs_3Bi_2I_9$ showed poor performance, whereas the I-V curve of $Cs_3Bi_2I_6Br_3$ showed improved performance. The highest PCE of 1.15% was achieved for the $Cs_3Bi_2I_6Br_3$-based perovskite solar cells. The integrated J_{sc} for the $Cs_3Bi_2I_6Br_3$-based perovskite solar cells has been presented in **Figure 10b**, which showed the J_{sc} value of 3.11 mA/cm^2. However, the PCE of 0.23% was obtained for the $Cs_3Bi_2I_9$-based perovskite solar cell device. The enhanced performance of the $Cs_3Bi_2I_6Br_3$-based perovskite solar cells attributed to the lower band gap and higher absorption property of $Cs_3Bi_2I_6Br_3$ perovskite structure.

These obtained PCE were quite interesting, which is believed due to the tuning of the perovskite structure and better absorption activity of the $Cs_3Bi_2I_6Br_3$. Further improvements are still required to enhance the performance of the bismuth-based perovskite solar cells.

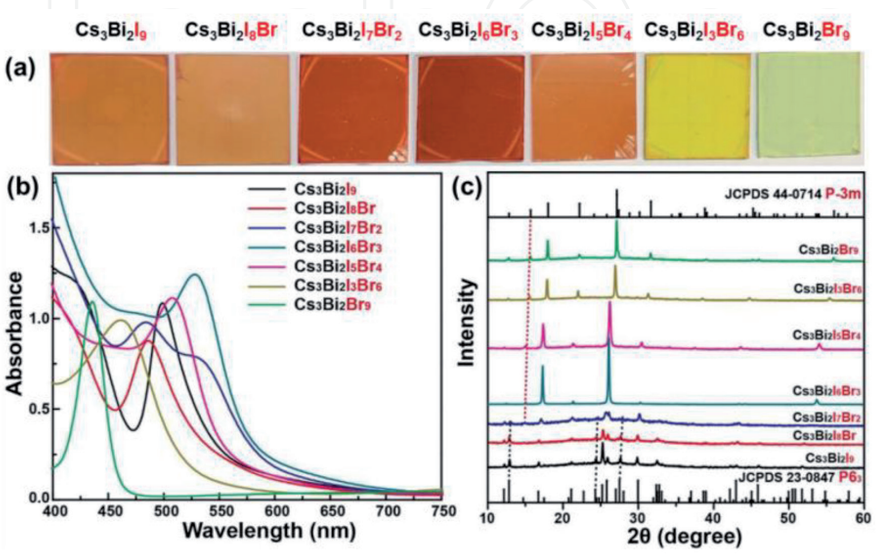

Figure 8.
Optical images (a), UV-vis spectra (b) and XRD patterns of $Cs_3Bi_2I_{9-x}Br_x$ (x = 0, 1, 2, 3, 4, 6 and 9). Reproduced with permission [39].

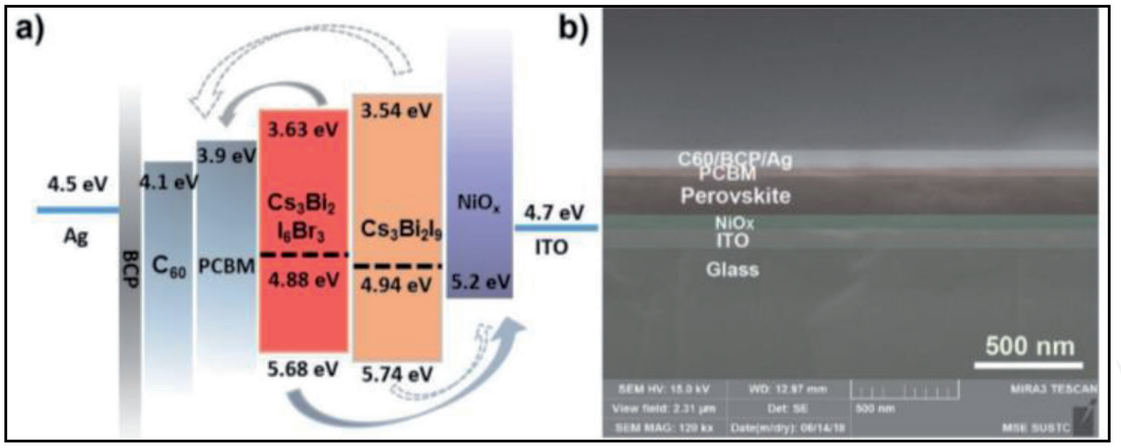

Figure 9.
Energy level graph (a) and cross-sectional SEM image (b) of perovskite solar cells. Reproduced with permission [39].

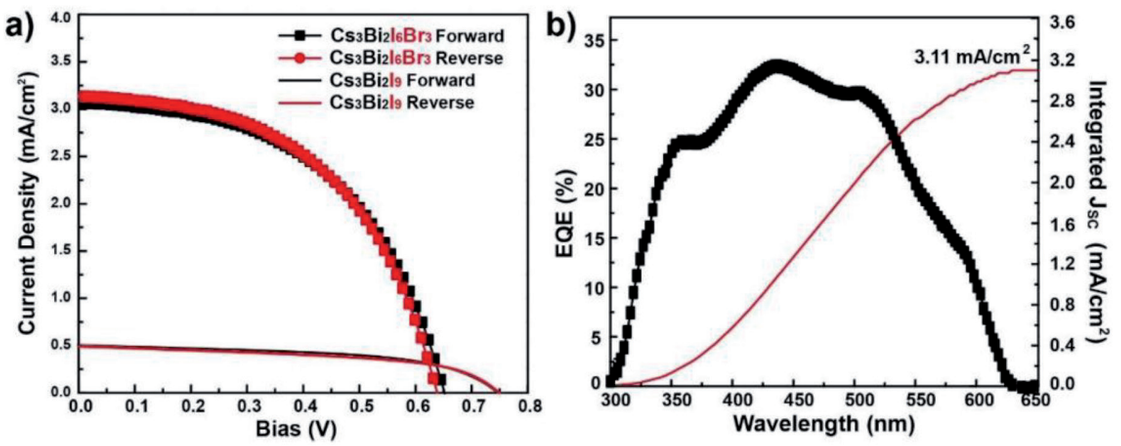

Figure 10.
I-V curves (a) and EQE (b) of the fabricated perovskite solar cells. Reproduced with permission [39].

4. Future prospective

It is well understood that Pb-based solar cells could not be commercialized due to the poor stability and toxic nature of Pb. Thus, Bi-based perovskite solar cells were developed under benign approaches as listed in **Table 1**. Since 2017, various approaches were made to construct the highly stable Pb-free PSCs. In this regard, Ghasemiet et al. [37] prepared $(PEA)_3Bi_2I_9$ perovskite light absorber and constructed the PSC device. The developed device exhibited PCE of 0.3%. Kulkarni

S. No.	Light absorbers	J_{sc} (mA/cm^2)	V_{oc} (mV)	PCE (%)	References
1.	$(PEA)_3Bi_2I_9$	~0.81	614	0.3	[37]
2.	$(MA)_3Bi_2I_9$	~0.4	515	0.09	[37]
3.	$(MA)_3Bi_2I_9$	~0.87	530	0.3	[38]
4.	$Cs_3Bi_2I_6Br_3$	3.11	~650	1.15	[39]
5.	$Cs_3Bi_2I_9$	~0.501	~750	0.23	[39]

Table 1.
Photovoltaic parameters of Bi-based perovskite solar cells.

et al. [38] also employed novel and unique approaches to improve the surface morphology of the $(MA)_3Bi_2I_9$ perovskite film, and the developed PSC device showed PCE of 0.3%. Yu et al. [39] also tuned the optical properties of the $Cs_3Bi_2I_9$ perovskite structure. Thus, the designed and synthesized $Cs_3Bi_2I_6Br_3$ perovskite material-based PSC device showed enhanced PCE of 1.15%. These obtained results showed the excellent optical properties of the Bi-based perovskite materials and suggested their potential as light absorbers in the construction of PSCs.

The Bi-based perovskite structures have wide band gap ~2.2 eV, which limits their absorption properties. Moreover, poor surface morphology of the Bi-based perovskite structures has been the other drawback, which resulted in the poor performance. Hence, the following strategies could be the key points to further improve the performance of the Bi-based perovskite solar cells:

1. Introducing new device architecture of the perovskite solar cells may improve the performance of the perovskite solar cells.

2. The performance of the Bi-based perovskite solar cells could be enhanced by developing the novel charge extraction/electron transport layer.

3. Some new approaches can be applied to prepare the high-quality thin films of the Bi-based perovskite structures, which further help to improve the photovoltaic parameters.

4. Solvent engineering and doping of Bi-based perovskite structure may also improve the performance of the perovskite solar cells.

5. Conclusions

The origin and advances in the field of perovskite solar cells have been reviewed. Perovskite solar cells could be the future energy source with low cost. The replacements of the toxic Pb with different metals have been investigated to produce Pb-free perovskite structures for the development of Pb-free perovskite solar cells. Bismuth, which is a nontoxic element, has been widely employed for the development of highly stable and Pb-free perovskite structures. Bi-based perovskite structures have shown promising performance and their performance may be further improved by incorporating unique approaches and efficient charge extraction layers.

Acknowledgements

K.A. sincerely acknowledged Discipline of Chemistry, IIT Indore. K.A. also thanks UGC, New Delhi, India, for RGNFD fellowship.

Conflict of interest

The author declares no conflict of interest.

IntechOpen

Author details

Khursheed Ahmad
Discipline of Chemistry, Indian Institute of Technology Indore, Simrol, M.P., India

*Address all correspondence to: khursheed.energy@gmail.com

IntechOpen

References

[1] Sum TC, Mathews N. Advancements in perovskite solar cells: Photophysics behind the photovoltaics. Energy & Environmental Science. 2014;**7**:2518-2534

[2] Reddy VS, Kaushik SC, Ranjan KR, Tyagi SK. State-of-the-art of solar thermal power plants. Renewable and Sustainable Energy Reviews. 2013;**27**:258-273

[3] Kitano M, Hara M. Heterogeneous photocatalytic cleavage of water. Journal of Materials Chemistry. 2010;**20**:627-641

[4] Ahmad K, Mobin SM. Graphene oxide based planar heterojunction perovskite solar cell under ambient condition. New Journal of Chemistry. 2017;**41**:14253-14258

[5] Chen Y-Z, Wu R-J, Lin LY, Chang WC. Novel synthesis of popcorn-like TiO2 light scatterers using a facile solution method for efficient dye-sensitized solar cells. Journal of Power Sources. 2019;**413**:384-390

[6] Kojima A, Teshima K, Shirai Y, Miyasaka T. Organometal halide perovskites as visible-light sensitizers for photovoltaic cells. Journal of the American Chemical Society. 2009;**131**:6050-6051

[7] Ahmad K, Mohammad A, Mobin SM. Hydrothermally grown α-MnO2 nanorods as highly efficient low cost counter-electrode material for dye-sensitized solar cells and electrochemical sensing applications. Electrochimica Acta. 2017;**252**:549-557

[8] Im JH, Lee CR, Lee JW, Park SW, Park NG. 6.5% efficient perovskite quantum-dot-sensitized solar cell. Nanoscale. 2011;**3**:4088-4093

[9] Kim HS, Lee CR, Im JH, Lee KB, Moehl T, Marchioro A, et al. Lead iodide perovskite sensitized all-solid-state submicron thin film mesoscopic solar cell with efficiency exceeding 9%. Scientific Reports. 2012;**2**:591

[10] Wehrenfennig C, Liu M, Snaith HJ, Johnston MB, Herz LM. Charge-carrier dynamics in vapour-deposited films of the organolead halide perovskite CH3NH3PbI3−xClx. Energy & Environmental Science. 2014;**7**:2269-2275

[11] Ma J, Guo X, Zhou L, Lin Z, Zhang C, Yang Z, et al. Enhanced planar perovskite solar cell performance via contact passivation of TiO2/perovskite interface with NaCl doping approach. ACS Applied Energy Materials. 2018;**1**:3826-3834

[12] Ke W, Fang G, Wang J, Qin P, Tao H, Lei H, et al. Perovskite solar cell with an efficient TiO2 compact film. ACS Applied Materials & Interfaces. 2014;**6**:15959-15965

[13] Guo Z, Liguo G, Zhang C, Xu Z, Ma T. Low-temperature processed non-TiO2 electron selective layers for perovskite solar cells. Journal of Materials Chemistry A. 2018;**6**:4572-4589

[14] Peng G, Wu J, Wu S, Xu X, Ellis JE, Xu G, et al. Perovskite solar cells based on bottom-fused TiO2 nanocones. Journal of Materials Chemistry A. 2016;**4**:1520-1530

[15] Lv M, Lv W, Fang X, Sun P, Lin B, Zhang S, et al. Performance enhancement of perovskite solar cells with a modified TiO2 electron transport layer using Zn-based additives. RSC Advances. 2016;**6**:35044-35050

[16] Liu D, Kelly TL. Perovskite solar cells with a planar heterojunction structure prepared using room-temperature solution processing techniques. Nature Photonics. 2014;**8**:133-138

[17] Jeong S, Seo S, Park H, Shin H. Atomic layer deposition of a SnO2 electron-transporting layer for planar perovskite solar cells with a power conversion efficiency of 18.3%. Chemical Communications. 2019;**55**:2433-2436

[18] Wang S, Zhu Y, Liu B, Wang C, Ma R. Introduction of carbon nanodots into SnO2 electron transport layer for efficient and UV stable planar perovskite solar cells. Journal of Materials Chemistry. 2019;**7**:5353-5362

[19] Ding B, Huang SY, Chu QQ, Li Y, Li CX, Li CJ, et al. Low-temperature SnO2-modified TiO2 yields record efficiency for normal planar perovskite solar modules. Journal of Materials Chemistry A. 2018;**6**:10233-10242

[20] Lee MM, Teuscher J, Miyasaka T, Murakami TN, Snaith HJ. Efficient hybrid solar cells based on meso-superstructured organometal halide perovskites. Science. 2012;**338**:643-647

[21] Zimmermann I, Aghazad S, Nazeeruddin MK. Lead and HTM free stable two-dimensional tin perovskites with suitable band gap for solar cell applications. Angewandte Chemie, International Edition. 2019;**131**:1084-1088

[22] He M, Chen Y, Liu H, Wang J, Fang X, Liang Z. Chemical decoration of $CH_3NH_3PbI_3$ perovskites with graphene oxides for photodetector applications. Chemical Communications. 2015;**51**:9659-9661

[23] Xu JT, Chen YH, Dai LM. Efficiently photo-charging lithium-ion battery by perovskite solar cell. Nature Communications. 2015;**6**:8103

[24] Tathavadekar M, Krishnamurthy S, Banerjee A, Nagane S, Gawli Y, Suryawanshi A, et al. Low-dimensional hybrid perovskites as high performance anodes for alkali-ion batteries. Journal of Materials Chemistry A. 2017;**5**:18634-18642

[25] Leyden MR, Meng L, Jiang Y, Ono L, Qiu EJ, Juarez-Perez C, et al. Methylammonium lead bromide perovskite light-emitting diodes by chemical vapor deposition. Journal of Physical Chemistry Letters. 2017;**8**:3193-3198

[26] Xu X, Li S, Zhang H, Shen Y, Zakeeruddin SM, Graetzel M, et al. A power pack based on organometallic perovskite solar cell and supercapacitor. ACS Nano. 2015;**9**:1782-1787

[27] Krishnamoorthy T, Ding H, Yan C, Leong WL, Baikie T, Zhang Z, et al. Lead-free germanium iodide perovskite materials for photovoltaic application. Journal of Materials Chemistry A. 2015;**3**:23829-23832

[28] Koh TM, Krishnamoorthy T, Yantara N, Shi C, Leong WL, Boix PP, et al. Formamidinium tin-based perovskite with low Eg for photovoltaic applications. Journal of Materials Chemistry A. 2015;**3**:14996-15000

[29] Ahmad K, Kumar P, Mobin SM. A two-step modified sequential deposition method-based Pb-free (CH3NH3)3Sb2I9 perovskite with improved open circuit voltage and performance. ChemElectroChem. 2020;**7**:946-950

[30] Ahmad K, Ansari SN, Natarajan K, Mobin SM. A two-step modified deposition method based (CH3NH3)3Bi2I9 perovskite: Lead free, highly stable and enhanced photovoltaic performance. ChemElectroChem. 2019;**6**:1-8

[31] Ahmad K, Ansari SN, Natarajan K, Mobin SM. Design and Synthesis of 1D-Polymeric Chain Based [(CH3NH3)3Bi2Cl9]n Perovskite: A New Light Absorber Material for Lead Free Perovskite Solar Cells. ACS Applied Energy Materials. 2018;**01**:2405-2409

[32] Ahmad K, Mobin SM. Organic–Inorganic Copper (II)-Based

Perovskites: A Benign Approach toward Low-Toxicity and Water-Stable Light Absorbers for Photovoltaic Applications. Energy Technology. 2019. DOI: 10.1002/ente.201901185

[33] Park BW, Philippe B, Zhang X, Rensmo H, Boschloo G, Johansson EMJ. Bismuth based hybrid perovskites $A_3Bi_2I_9$ (a: Methylammonium or cesium) for solar cell application. Advanced Materials. 2015;**27**:6806

[34] Shin SS, Correa Baena JP, Kurchin RC, Polizzotti A, Yoo JJ, Wieghold S, et al. Solvent-engineering method to deposit compact bismuth-based thin films: Mechanism and application to photovoltaics. Chemistry of Materials. 2018;**30**:336-343

[35] Jain SM, Phuyal D, Davies ML, Li M, Philippe B, De Castro C, et al. An effective approach of vapour assisted morphological tailoring for reducing metal defect sites in lead-free, (CH3NH3)(3)Bi2I9 bismuth-based perovskite solar cells for improved performance and long-term stability. Nano Energy. 2018;**49**:614-624

[36] Lan C, Liang G, Zhao S, Lan H, Peng H, Zhang D, et al. Lead-free formamidinium bismuth perovskites (FA)3Bi2I9 with low bandgap for potential photovoltaic application. Solar Energy. 2019;**177**:501-507

[37] Ghasemi M, Lyu M, Roknuzzaman M, Yun JH, Hao M, He D, et al. Phenethylammonium bismuth halides: from single crystals to bulky-organic cation promoted thin-film deposition for potential optoelectronic applications. Journal of Materials Chemistry A. 2019;7:20733-20741

[38] Kulkarni A, Singh T, Ikegami M, Miyasaka T. Photovoltaic enhancement of bismuth halide hybrid perovskite by N-methyl pyrrolidone-assisted morphology conversion. RSC Advances. 2017;7:9456-9460

[39] Yu BB, Li M, Yang J, Chen W, Zhu Y, Zhang X, et al. Alloy-induced phase transition and enhanced photovoltaic performance: The case of Cs3Bi2I9-xBrx perovskite solar cells. Journal of Materials Chemistry A. 2019;7:8818-8825